Model-based predictive control for bicycling in urban intersections

C. Portilla [a,*], F. Valencia [a,b], J. Espinosa [a], A. Núñez [c], B. De Schutter [d]

[a] Facultad de Minas, Universidad Nacional de Colombia, Medellín, Colombia
[b] Solar Energy Research Center SERC-Chile, Faculty of Mathematical and Physical Sciences, University of Chile, Chile
[c] Section of Railway Engineering, Delft University of Technology, Delft, The Netherlands
[d] Delft Center for Systems and Control, Delft University of Technology, Delft, The Netherlands

ARTICLE INFO

ABSTRACT

In this paper, a model predictive control approach for improving the efficiency of bicycling as part of intermodal transportation systems is proposed. Considering a dedicated bicycle lanes infrastructure, the focus in this paper is to optimize the dynamic interaction between bicycles and vehicles at the multimodal urban traffic intersections. In the proposed approach, a dynamic model for the flows, queues, and number of both vehicles and bicycles is explicitly incorporated in the controller. For obtaining a good trade-off between the total time spent by the cyclists and by the drivers, a Pareto analysis is proposed to adjust the objective function of the MPC controller. Simulation results for a two-intersections urban traffic network are presented and the controller is analyzed considering different methods of including in the MPC controller the inflow demands of both vehicles and bicycles.

1. Introduction

Congestion in urban areas is one of the biggest issues of modern society. It has several negative environmental, economical, and health impacts. Thus, it is essential to develop adequate transportation systems to mitigate the effects of congestion and to increase the sustainable development of every city. Good solutions will heighten environmental sustainability, yield societal benefits, and reduce energy problems. Given the importance of mobility different approaches have been proposed (Shen and Zhang, 2014; Budnitzki, 2014; Fahad et al., 2014) to diminish the impacts associated with congestion. In particular, in Schmöcker et al. (2008), Li et al. (2014), and Zhang et al. (2013) optimization-based approaches for urban congestion management have been studied, considering real urban scenarios and environmental concerns. However, cycling has emerged strongly in the last years as an alternative transportation mode, and it needs to be explicitly considered in signal timing design.

The benefits of using bicycles are numerous (Gatersleben and Haddad, 2010). The use of a bicycle on a regular basis can play an important role as a mode of transportation, while also addressing climate change problems, and obtaining energy, health, economic, and quality of life benefits. For short journeys, the use of bicycles instead of motorized forms of transport can help to reduce the overall level of fuel consumption, while also decreasing emissions from cold starts caused by short car trips. Bicyclists can often bypass congestion and grid-locked traffic, and in some instances may even arrive at their

---

* Corresponding author.
  E-mail addresses: crportil@unal.edu.co (C. Portilla), felipe.valencia@sercchile.cl (F. Valencia), jespinov@unal.edu.co (J. Espinosa), a.a.nunezvicencio@tudelft.nl (A. Núñez), b.deschutter@tudelft.nl (B. De Schutter).

destinations faster than if they had driven a car. In many countries, the cost of owning and operating a car can account for almost 18% of a typical household's income, so bicycling can provide options also for those who would like to save money (U. S. Department of Transportation, 2010). In addition, regular bicycling is an important form of exercise, which is relevant to reduce risk of coronary heart disease, stroke, diabetes, health costs, and to improve quality of life for people of all ages. However, the growing use of the bicycles has generated new challenges (Cheng et al., 2008; Dijkstra, 2012; Guizhu and Bing, 1997; Parkin and Meyers, 2010). For instance, the intense competition between cyclists and drivers (Fig. 1), for the common spaces in the urban traffic network has consequences in the way urban mobility has been conceived so far. While "pro-bike" users demand for higher safety measures and priority, these measures might go in detriment of the other transportation modes that compete for the use of space, at for instance the traffic intersections.

In order to cope with the new challenges, the design of new control strategies that take into account the interaction between the vehicles and the arising transportation modes is mandatory. In He et al. (2014), He et al. (2012), Cesme and Furth (2014), and Guler et al. (2014) different approaches were proposed for the control of transportation networks with several transportation modes. Additionally, in Wu and Liu (2014) an overview of methodologies towards an effective use of high-resolution data for traffic modeling and control purposes is presented. In this paper, we consider the use of a model-based predictive control approach (Camacho and Bordons, 1999), since in such a control technique the synergies among the dynamics of the system are exploited to optimize a general performance criterion that can include multiple objectives (Burger et al., 2013).

In the literature, dynamic models representing the behavior of the flow of vehicles in urban environments can be found in van den Berg et al. (2003), van den Berg et al. (2004), Hegyi et al. (2005), Daganzo (1995), and Le et al. (2013). However, in the case of bicycle flows, those models are rare. In fact, to the authors' best knowledge the interaction between the two flows (vehicles and bikes) has not been addressed yet. In this paper a dynamic model for the traffic of bicycles is proposed. Such model is based on the S model of Lin et al. (2012), and improved by Jamshidnejad et al. (submitted for publication). Based on this model, the dynamic interaction between bikes and vehicles is defined and included in the controller. Hence, both flows can be regulated under the influence of each other. The proposed model is tested for a network consisting of two multimodal traffic light intersections. The performance of the MPC controller is compared with a state-feedback control scheme and a fixed-time strategy. We conclude the MPC controller performs better than the other controllers when a good estimation of the inflow demands of both vehicles and bicycles is available.

The next sections of this paper are organized as follows: In Section 2 the urban traffic and the bicycle traffic model are presented. Then, in Section 3 the formulation of a centralized model predictive controller and of a non-linear state-feedback controller is presented. Section 4 presents the interaction between these two models and simulation results. Finally, in Section 5 concluding remarks are presented.

2. Multi-modal traffic model

2.1. Urban traffic model

In this section, the S model (Lin et al., 2011) is considered to represent the behavior of urban traffic. This model is a simplified version of the BLX model described in Lin et al. (2012), which is itself a modified version of the model proposed by van den Berg et al. (2003). The extended version of the S model capable to consider congestion and emission is described in Jamshidnejad et al. (submitted for publication). The main advantage of the S model over the others is its reduced computational burden and its degree of representation of the real system, which is similar to that of more complex models. Therefore, it is better suited for use in real-time to control systems. In the S model, a link (u, d) represents a road between intersection u and intersection d as shown in Fig. 2. In this model two states are considered at every time step k_d: the total number of vehicles $\eta_{u,d}^v(k_d)$, and the number of vehicles $q_{u,d,o}^v(k_d)$ waiting in the queue turning to the direction o (it could be a left-turn, right-turn, or straight-through queue).
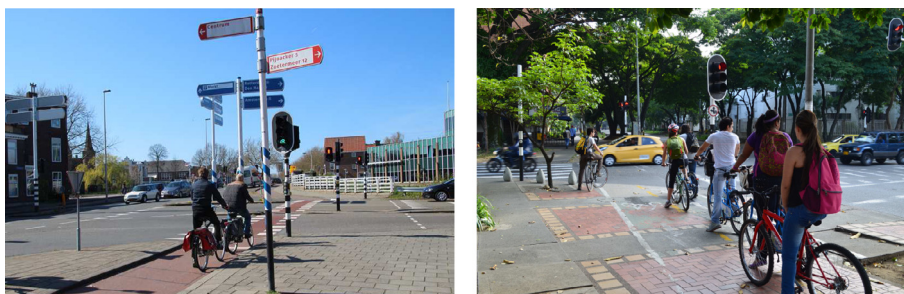
(a) Bicycle road in Delft - Netherlands   (b) Bicycle road in Medellin - Colombia

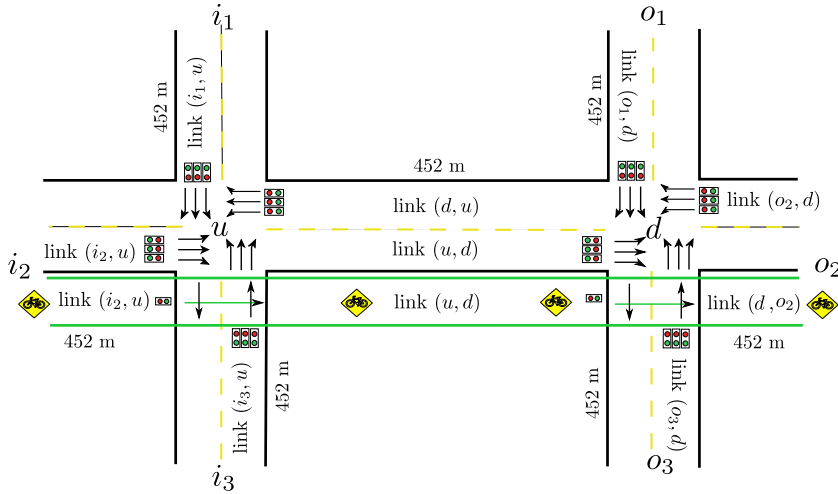Fig. 1. Examples of bicycle roads around the world.

Fig. 2. Two interconnected intersections in an urban traffic network.

The mathematical model describing the behavior of the urban traffic is determined by the following equations:

$$\eta_{u,d}^{v}(k_d + 1) = \eta_{u,d}^{v}(k_d) + \left(\alpha_{u,d}^{v_{\text{enter}}}(k_d) - \alpha_{u,d}^{v_{\text{leave}}}(k_d)\right)c_d, \tag{1}$$

$$q_{u,d,o}^{v}(k_d + 1) = q_{u,d,o}^{v}(k_d) + \left(\alpha_{u,d,o}^{v_{\text{arriv}}}(k_d) - \alpha_{u,d,o}^{v_{\text{leave}}}(k_d)\right)c_d, \tag{2}$$

$$\alpha_{u,d}^{v_{\text{enter}}}(k_d) = \sum_{i \in I_{u,d}^{v}} \alpha_{i,u,d}^{v_{\text{leave}}}(k_d), \tag{3}$$

$$\alpha_{u,d}^{v_{\text{leave}}}(k_d) = \sum_{o \in O_{u,d}^{v}} \alpha_{u,d,o}^{v_{\text{leave}}}(k_d), \tag{4}$$

$$\alpha_{u,d,o}^{v_{\text{leave}}}(k_d) = \min\left\{ \frac{\mu_{u,d,o}^{v} g_{u,d,o}^{v}(k_d)}{c_d}, \frac{q_{u,d,o}^{v}(k_d)}{c_d} + \alpha_{u,d}^{v_{\text{arriv}}}(k_d), \frac{\beta_{u,d,o}^{v}(k_d)(C_{d,o}^{v} - \eta_{d,o}^{v}(k_d))}{\sum_{u \in I_{d,o}^{v}} \beta_{u,d,o}^{v}(k_d)c_d} \right\}, \tag{5}$$

$$\alpha_{u,d,o}^{v_{\text{arriv}}}(k_d) = \beta_{u,d,o}^{v}(k_d)\,\alpha_{u,d}^{v_{\text{arriv}}}(k_d), \tag{6}$$

$$\alpha_{u,d}^{v_{\text{arriv}}}(k_d) = \frac{c_d - \gamma_{u,d}^{v}(k_d)}{c_d}\alpha_{u,d}^{v_{\text{enter}}}(k_d - \tau_{u,d}^{v}(k_d)) + \frac{\gamma_{u,d}^{v}(k_d - 1)}{c_d}\alpha_{u,d}^{v_{\text{enter}}}(k_d - \tau_{u,d}^{v_{\text{arriv}}}(k_d - 1) - 1), \tag{7}$$

$$\tau_{u,d}^{v}(k_d) = \text{floor}\left\{ \frac{\left(C_{u,d}^{v} - q_{u,d}^{v}(k_d)\right)l^{v}}{N_{u,d}^{v_{\text{lane}}} v_{u,d}^{v_{\text{free}}} c_d} \right\}, \tag{8}$$

$$\gamma_{u,d}^{v}(k_d) = \text{rem}\left\{ \frac{\left(C_{u,d}^{v} - q_{u,d}^{v}(k_d)\right)l^{v}}{N_{u,d}^{v_{\text{lane}}} v_{u,d}^{v_{\text{free}}}}, c_d \right\}, \tag{9}$$

$$q_{u,d}^{v}(k_d) = \sum_{o \in O_{u,d}^{v}} q_{u,d,o}^{v}(k_d). \tag{10}$$

The parameters $c_d, \mu_{u,d,o}^{v}, g_{u,d,o}^{v}(k_d), \beta_{u,d,o}^{v}(k_d), \eta_{d,o}^{v}(k_d)$, and $C_{d,o}^{v}$ represent the cycle time, peak flow, green time of the traffic light, the split ratio, the number of vehicles in link (d, o) at step k_d, and the link capacity (d, o) respectively. Moreover, $l^{v}, N_{u,d}^{v_{\text{lane}}}, C_{u,d}^{v}$ and $v_{u,d}^{v_{\text{free}}}$ are the average length of the vehicles, the number of lanes in link (u, d), the link capacity, and the free flow rate. In addition, $O_{u,d}^{v}$ and $I_{u,d}^{v}$ are the output and input nodes from link (u, d). The variable $\alpha_{u,d}^{v_{\text{enter}}}(k_d)$ is the flow rate entering link (u, d)

at time step k_d and $\alpha_{u,d}^{v\text{leave}}(k_d)$ is the leaving average flow rate at time step k_d. The flow rate leaving (u, d) to the direction o is denoted by $\alpha_{u,d,o}^{v\text{leave}}(k_d)$, and $\alpha_{u,d,o}^{v\text{arriv}}(k_d)$ is the arrival flow at tail of queue after a time delay $\tau_{u,d}^v(k_d)c_d + \gamma_{u,d}^v(k_d)$.

2.2. Bicycle traffic model

In Section 2.1, the S model for urban traffic was introduced. Now, the S model is used to derive a dynamic model for bicycling. With this aim, consider the bicycle path shown in Fig. 2. In this path, the interaction between vehicles and bicycles is assumed to happen only at the traffic lights. That is, the scheduling of the traffic lights determines the behavior of the queues of vehicles and bicycles. Note that our layout will only hold if bikes are in the right hand side beside the road, in a cycle path. Let the pair (u, d) denote a road between an intersection u to another intersection d on the bicycle road. At every time step k_d, let $\eta_{u,d}^b(k_d)$ be the number of bicycles and $q_{u,d,o}^b(k_d)$ be the number of bicycles waiting in the queue turning to the direction o. From the flow balance at each link, the change in the number of bicycles at each link is determined by

$$\eta_{u,d}^b(k_d + 1) = \eta_{u,d}^b(k_d) + \left(\alpha_{u,d}^{b\text{enter}}(k_d) - \alpha_{u,d}^{b\text{leave}}(k_d)\right)c_d, \tag{11}$$

where $\alpha_{u,d}^{b\text{enter}}(k_d)$ and $\alpha_{u,d}^{b\text{leave}}(k_d)$ denote the average input and output flows at time step k_d, with:

$$\alpha_{u,d}^{b\text{enter}}(k_d) = \sum_{i \in I_{u,d}^b} \alpha_{i,u,d}^{b\text{leave}}(k_d), \tag{12}$$

$$\alpha_{u,d}^{b\text{leave}}(k_d) = \min\left\{\frac{\mu_{u,d}^b g_{u,d}^b(k_d)}{c_d}, \frac{q_{u,d}^b(k_d)}{c_d}\right\}, \tag{13}$$

with $\mu_{u,d}^b$ and $g_{u,d}^b(k_d)$ representing the maximum flow of bicycles and the green time of the traffic light at time step k_d; $I_{u,d}$ being the set of incoming flows of link (u, d), and $\alpha_{u,d,o}^{b\text{leave}}(k_d)$ being the leaving average flow rate of bicycles, i.e.,

$$\alpha_{u,d,o}^{b\text{leave}}(k_d) = \beta_{u,d,o}^b(k_d)\alpha_{u,d}^{b\text{leave}}(k_d), \tag{14}$$

where $\beta_{u,d,o}^b(k_d)$ is the fraction the bicycles leaving the link (u, d) and turning to o. Also, $q_{u,d}^b(k_d)$ is defined as:

$$q_{u,d}^b(k_d + 1) = q_{u,d}^b(k_d) + \left(\alpha_{u,d}^{b\text{arriv}}(k_d) - \alpha_{u,d}^{b\text{leave}}(k_d)\right)c_d. \tag{15}$$

In (15), the superscript arriv denotes the arrival flow. Then $\alpha_{u,d}^{b\text{arriv}}(k_d)$ is the arrival flow of bicycles to the link (u, d) and is defined as:

$$\alpha_{u,d}^{b\text{arriv}}(k_d) = \alpha_{u,d}^{b\text{enter}}(k_d - \tau_{u,d}^b(k_d)), \tag{16}$$

where

$$\tau_{u,d}^b(k_d) = \text{round}\left\{\frac{C_{u,d}^b - q_{u,d}^b(k_d)}{l^b \, v_{u,d}^{b\text{free}} \, c_d}\right\}, \tag{17}$$

is the delay of the flow arriving to the tail of the queue, with $q_{u,d}^b(k_d)$, $C_{u,d}^b$, l^b, and $v_{u,d}^{b\text{free}}$ the bicycles waiting to go to link (u, d), the capacity of the link (u, d), the average length of the bicycles, and the free flow speed, respectively.

Note that the vehicle and bicycle models have some differences. These differences are:

1. The output flow for vehicles (5) depends on the available space in the downstream link. However, since in the case of bicycles it is assumed that they can be accommodated in smaller spaces, the output flow (13) does not consider the available space in the downstream link.
2. The arrival flow of vehicles (7) corresponds to an exact discretization of a system with delay, this equation has two terms; a floor approximation and its remnant. However, in the arrival flow of bicycles, the delay was simplified in (16) because we assume that rounding delay was enough to describe the dynamic behavior of bicycles in our case study. Usually simple models are more handy for real-life MPC implementations; however, since the vehicle model is still complex, the total CPU time reduction expected is not that high. As bicycle flow theory is in its infancy, we expect that nearly in the future more detailed models will be made available and they can be compared using the MPC framework in terms of accuracy and control performance.

In the next section two model-based control strategies are proposed, namely, a state-feedback and a model predictive control strategy. Since both control strategies demand the use of a model, the S model and the bicycling model are used in their designs.

3. Controller design

3.1. State feedback control

State feedback control is a control strategy in which the control actions depend on the values of the system states. Due to its simplicity, this control strategy is widely used in applications involving multiple-input multiple-output systems. By its nature, state feedback control is reactive, that is, once the state trajectories deviate from their desired values, a control action is produced. In the case of traffic control, the implementation of an state feedback controller implies the measurement of the queue lengths associated to each stage.

Let $x(k_d) = [x_v^T(k_d), \; x_b^T(k_d)]^T$ and $u(k_d) = \left[\left(g_{u,d,o}^v(k_d) \right)^T, \; \left(g_{u,d,o}^b(k_d) \right)^T \right]^T$ be the state vector for all the links and the vector of inputs respectively, where $x_v(k_d) = \left[\left(\eta_{u,d}^v(k_d) \right)^T, \; \left(q_{u,d,o_1}^v(k_d) \right)^T, \; \left(q_{u,d,o_2}^v(k_d) \right)^T, \; \left(q_{u,d,o_3}^v(k_d) \right)^T \right]^T$, where T is the transpose operator, and $x_b(k_d) = \left[\left(\eta_{u,d}^b(k_d) \right)^T, \; \left(q_{u,d}^b(k_d) \right)^T \right]^T$. Then, the following control law is proposed:

$$u_f(k_d + 1) = u_f(k_d) - k_f \, q_{T_f}(k_d) - k_{\hat{f}} \, q_{T_{\hat{f}}}(k_d), \tag{18}$$

where k_f and $k_{\hat{f}}$ are constant, $u_f(k_d)$ is the green time of the traffic light for stage f and $u_{\hat{f}}$ is the total time for all other stages. The proposed control law is updated considering a weighted sum of the number of bikes and the number of vehicles waiting in the intersection. The control action is thus updated in accordance with its previous value and the result of the weighted sum. In (18) $q_{T_f}(k_d)$ is the queue associated to stage f and $q_{T_{\hat{f}}}(k_d)$ is the total queue associated to the others stages $\hat{f}$:

$$q_{T_f}(k_d) = \sum_{n \in U_f} q_n(k_d), \tag{19}$$

$$q_{T_{\hat{f}}}(k_d) = \sum_{m \in U_{\hat{f}}} q_m(k_d), \tag{20}$$

where U_f and $U_{\hat{f}}$ are the sets the lanes related with each one of the stages.

Let $\Delta u_f(k_d)$ be the change in the control actions $(\Delta u_f(k_d) = u_f(k_d) - u_f(k - 1))$, K_f be the vector of gains, i.e, $K_f = \left[k_f^T, \; k_{\hat{f}}^T \right]^T$ and Q_f be the vector of queue lengths, i.e. $Q_f(k_d) = \left[q_{T_f}^T(k_d), \; q_{T_{\hat{f}}}^T(k_d) \right]^T$. Then from (18):

$$\Delta u_f(k_d) = K_f \, Q_f(k_d) \tag{21}$$

Note that $Q_f(k_d)$ can be expressed as a function of the states as:

$$Q_f(k_d) = C_f \, x(k_d) \tag{22}$$

where C_f is a vector whose entries are equal to one if the state is a queue and zero otherwise. Thus, (21) is equivalently rewritten as:

$$\Delta u(k_d) \equiv K \, C \, x(k_d) \tag{23}$$

with C a matrix whose rows are the C_f vectors and K a matrix whose rows are the K_f vectors.

3.2. Centralized model predictive control

Model predictive control (MPC) is an optimal control approach whose objective is to minimize a cost function inside a feasible region (Camacho and Bordons, 1999). This allows MPC to handle complex systems with input and state constraints, making such control scheme one of the most successful advanced control techniques implemented in industry only second to PID (Proportional-Integral-Derivative) control (Darby and Nikolaou, 2012; Lee, 2011).

MPC schemes rely on the model accuracy and also on the availability of sufficiently fast computational resources. Fig. 3 presents the procedures carried by an MPC controller. Given the current state, the behavior of the system is predicted over a prediction horizon of N_p time steps, assuming a control horizon of N_u possible changes in the control actions (one per time step), with $N_u \leqslant N_p$, as shown in Fig. 3(a). Taking into consideration the predicted behavior of the system, the possible variations in the control actions, the objective function of the controller, and the system constraints, an optimization procedure is carried out. As a consequence, a sequence of optimal control actions is obtained. From this sequence, the first element is applied to the system. This procedure is called receding horizon or moving horizon. Fig. 3(b) illustrates this procedure.

In the particular case of the traffic network shown in Fig. 2, at each sampling time step k_d the aforementioned procedure is carried out. In this case, the queues, number of vehicles, and number of bicycles waiting at an intersection are measured.
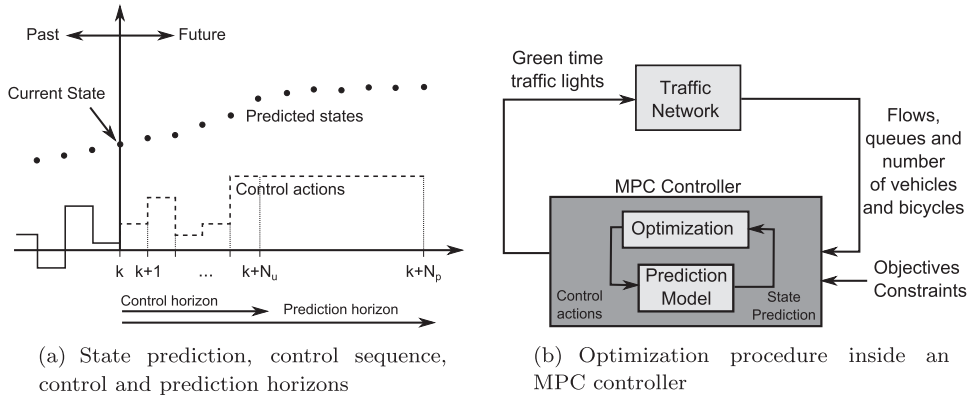
(a) State prediction, control sequence, control and prediction horizons

(b) Optimization procedure inside an MPC controller

Fig. 3. Procedures carried out inside an MPC controller.

With this information, and using the models described in Section 2, the behavior of the traffic network is predicted. Based on the predictions, the optimal green times for the traffic light that satisfy the system constraints, are computed.

Regarding the objective function, from the user point of view, when deciding which route to follow, the total travel time is not the only criterion. Many other variables often underestimated in traffic projects can be also considered in our approach, such as: safety, health benefits, stress, and pollution level. The MPC optimization problem at time step k_d is defined as follows:

$$\min_{U_{k_d}} J\left(U_{k_d}, x_v(k_d), x_b(k_d), D^v_{k_d}, D^b_{k_d}\right) \tag{24}$$

subject to

$$
\begin{aligned}
&x_v(k_d + t + 1) = f_v(x_v(k_d + t), u(k_d + t), v_v(k_d + t)) \\
&0 \leqslant \eta^v_{u,d}(k_d + t) \leqslant C^v_{u,d} \\
&0 \leqslant q^v_{u,d,o}(k_d + t), \quad \text{(vehicles)} \\
&x_b(k_d + t + 1) = f_b(x_b(k_d + t), u(k_d + t), v_b(k_d + t)) \\
&0 \leqslant \eta^b_{u,d}(k_d + t) \leqslant C^b_{u,d} \\
&0 \leqslant q^b_{u,d,o}(k_d + t), \quad \text{(bicycles)} \\
&0 \leqslant g_{u,d,o}(k_d + t - 1) \leqslant c_d \\
&\text{for} \quad t = 0, \ldots, N_p - 1, \quad (u, d) \in L, \quad o \in O
\end{aligned}
\tag{25}
$$

where J is the objective function, $x_v(k_d) = x^v_{k_d}, x_b(k_d) = x^b_{k_d}$ are defined as in Section 3.1; $D^v_{k_d} = [v^T_v(k_d), \ldots, v^T_v(k_d + N_p)]^T$ and $D^b_{k_d} = [v^T_b(k_d), \ldots, v^T_b(k_d + N_p)]^T$ are the predicted demand; $U_{k_d} = [u^T(k_d), \ldots, u^T(k_d + N_p - 1)]^T$ is the control sequence for the traffic signals at the intersections in L; $C^v_{u,d}$ and $C^b_{u,d}$ are the vehicle and bicycle capacity of a link (u, d) respectively.

In this particular approach, U_{k_d} is the sequence of green signal times $g_{u,d,o}(k_d)$ of all traffic lights in the network. The functions $f_v(\cdot)$ and $f_b(\cdot)$ are given by the S model including bicycling. Once the nonlinear optimization problem given by (24) and (25) is numerically solved, from the control sequence only the first control action $u(k_d)$ is applied at each intersection, and the same procedure is repeated for the next step $k_d + 1$ considering the new measurements (rolling horizon procedure).

For now, we consider just the total time spent (TTS) by bicycles and vehicles:

$$J(U_k, x_v(k_d), x_b(k_d)) = \sum_{t=1}^{N_p} \left(\alpha \sum_{(u,d) \in L} \eta^v_{u,d}(k_d + t)c_d + (1 - \alpha) \sum_{(u,d) \in L} \eta^b_{u,d}(k_d + t)c_d \right) \tag{26}$$

where α is a weight value that allows to privilege the vehicles traffic or the bicycles traffic, i.e, when $\alpha = 0.5$ the TTS of the vehicles will have the same importance as the TTS of the bicycles. The selection of α will change the overall performance in favor of the cyclists or in favor of the vehicles. A pro-bikes would prefer $\alpha = 0$, while a pro-vehicles would select $\alpha = 1$. In this paper, we propose a methodology that facilitate the visualization of the trade-offs between vehicles and bicycles, so that a traffic authority can have a well-informed final decision on a good α for the whole traffic network.

Note that the coupling of the vehicle and bicycle states is due to the control actions. This assumption is reasonable in cases where bicycles do not share the same road that vehicles as shown in Fig. 2. In these cases, the interaction between the two flows occurs because of the scheduling of the traffic lights.

The next section presents the simulation results obtained with the control strategies described throughout this section.

4. Simulation results

Here we present the results obtained when the model derived in Section 2 is used to design model-based control strategies such as MPC. As a benchmark, the urban traffic network shown in Fig. 2 is used. This traffic network is composed by two intersections, each of them with interaction between vehicles and bicycles. Both the flow of vehicles and the flow of bicycles are regulated by traffic lights. The parameters used in the simulations are: cycle time $c_d = 60$ s which is equal to the sampling time, initial value of 20 vehicles in each link and 5 vehicles at each input queue, initial value of 10 bicycles in each link and 0 bicycles at each input queue, length of each link 448 m, average length of each vehicle is 7 m, average length of each bicycle is 1.7 m, 3 lanes each link for vehicles and 1 lane for bicycles, free flow speed $v_{free} = 50$ km/h for vehicles and $v_{free} = 15$ km/h for bikes, the capacity of each link of vehicles is 192 and 264 for bicycles, and the maximum flow is 1800 veh/h/lane and 300 bikes/h.

Additionally, the inlet flow rate of vehicles and bicycles were considered time-dependent. The evolution of both inlet flow rates is shown in Fig. 4. In this figure, the label "Demand 1" stands for the inlet flow rates of vehicles at links (i_2, u) and (o_2, d), whereas the label "Demand 2" stands for the inlet flow rates of vehicles at links $(i_1, u), (i_3, u), (o_1, d)$ and (o_3, d) (Fig. 4(a)). Fig. 4(b) presents the time evolution of the inlet flow rate of bicycles at link (i_2, u).

In the simulation example the set of stages shown in Fig. 5 was used. Each stage in Fig. 5 defines the available set of directions. In stage 1 at intersection u, bicycles and vehicles are allowed to cross the intersection. In the same stage, vehicles on the link (u, d) and vehicles coming from (i_1, u) are also allowed to turn right. The stages proposed in this paper have the particularity that bicycles only are allowed to cross an intersection in stage 1. In this way, the remaining stages can be used to evacuate the vehicles waiting in the queues at each link. Moreover, a percentage of the sampling time c_d is assigned by the controller to each stage. Thereby, we assume all directions are allowed at least once every time step k_d. Then, the time assigned to each stage depends on how long c_d is. For model-based controllers, aspects such as the length of the queues and the expected travel time also influence the timing of each stage.

Fig. 6 presents the behavior of the number of vehicles and the number of bicycles in the intersection u of the network shown in Fig. 2. The result shown in Fig. 6 was obtained considering a time span of 12 h. Over this time span, it was assumed that all vehicles at (i_1, u) headed towards the link (u, i_3), and that only interaction between vehicles and bicycles appeared at links (i_1, u) and (i_2, u). The simulation was performed for different values of the green time assigned to the vehicles. As it can be noticed, as the green time assigned to the vehicles increases the number of vehicles in the queue decreases, whereas the number of bicycles rises. The opposite occurs when the green time assigned to the vehicles decreases.

Fig. 7 presents the TTS for the aforementioned 12 h simulations, as a function of the green time of stage 1. In this figure it is evident that as the time assigned to stage 1 increases the TTS decreases. However, increasing the time of stage 1 implies a reduction of the time of the remaining stages. Thereby, the TTS started to increase again, in all the cases analyzed, once the time assigned to stage 1 exceeded 16 s. This happened because reducing the time of stages 2, 3 and 4 produced an increase in the number of vehicles waiting on the corresponding links, which, as expected, implies an increase in the TTS. Indeed, if the times for stages 1–4 are considered fixed and equal to 15.8 s, 14 s, 16 s, and 14.2 s, respectively, the minimal TTS is obtained: 837.84 veh and bike.

Now, the performance of this control scheme is compared with those introduced in Section 3. The comparison is carried out assuming three different conditions on the demand shown in Fig. 4, namely, fixed, measured, and predictable demand (or fully-known in advance). These demand conditions affect the performance of the MPC controller, since only in this control strategy the demand is taken into account in the computation of the times for each stage. For MPC, a prediction horizon of 6 time steps and a control horizon of 3 were assumed. In addition to the state feedback (S.F.) controller, two other controllers are considered in the comparison. One is called open loop controller and uses the same green times for all the stages. The other controller is called fixed-time, which via an offline optimization the best fixed green times are assigned to all the stages during the whole simulation. The sections below present the simulation results.
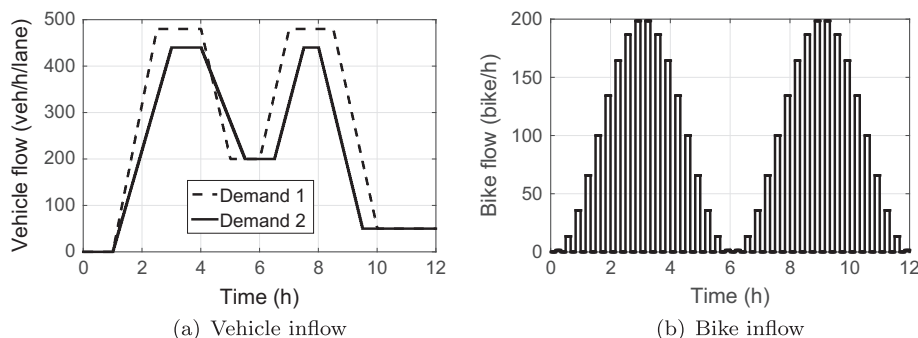

(a) Vehicle inflow   (b) Bike inflow

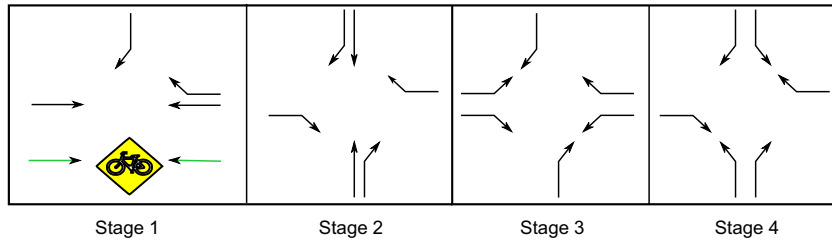**Fig. 4.** Inlet flow profile to the intersections.
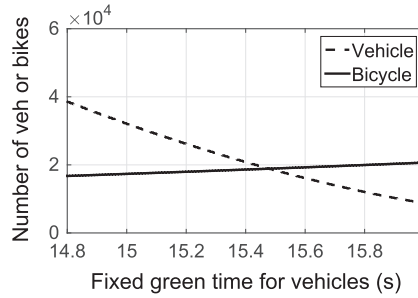
Fig. 5. Stages of the traffic lights.

Fig. 6. Number of vehicles and bikes as function of a fixed green time for vehicles at intersection u.
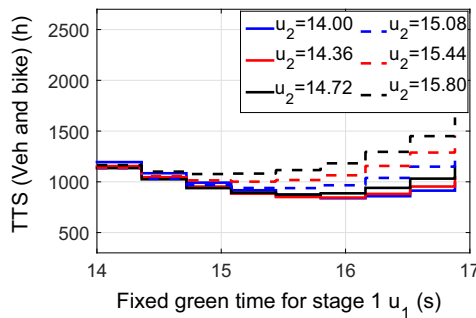

Fig. 7. TTS as function of a fixed green time of the stage 1 u_1 and 6 cases for the stage 2 u_2.

4.1. MPC Case 1: Constant demand

In this section, the performance of the state feedback and the MPC controller derived in Section 3 is compared with the performance of the controllers open loop and fixed-time.

Since MPC requires an estimation of the demand shown in Fig. 4, in MPC Case 1 was assumed that the predictive model of the demand is constant throughout the full simulation time. This case holds when there are not available sensors to measure of the inflow demands. Several values for the constant model of the demand were analyzed, from 0% to 300%, representing 100% the value of the average demand. The average values of Demand 1 and Demand 2 were 264.46 veh/h/lane and 215.78 veh/h/lane respectively. The average value of bicycles was 49.93 bike/h. Fig. 8 shows the total statistics for vehicles and bicycles for different constant demands assumed by the MPC controller. In Fig. 8(a) marked is the performance obtained when the demand is assumed 90% larger than the average. From the results presented in Fig. 8, it is evident that for the MPC controller the way the demand is incorporated has a high impact on the performance, in terms of the TTS and the time in queues (TQ). This is consistent with the claim that the performance of MPC controllers relies on the accuracy of the prediction model. Regarding the outlying points in Fig. 8, they suggest that using the nominal demand (100%) will reduce the performance of the controller, due to its underestimation of the demand during rush hours. Assuming a worst-case scenario, by fixing the demands near their historical maxima (200% or higher) will provide solutions that are too conservative, with a lower performance level than in the underestimated case (100% or lower). To mitigate this effect, the sensitivity analysis suggests to assume a demand higher than the average but a bit less than the maximum demand in rush hours, around 190%.

In addition, we must find the appropriate values for α in the objective function. Different values of α were analyzed and the results are shown in Fig. 9, all of them assuming the demand used by the MPC controller is constant and 90% larger than

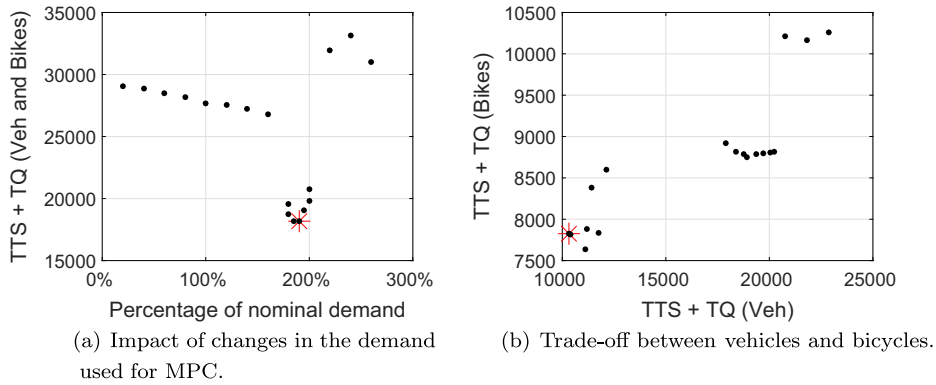(a) Impact of changes in the demand used for MPC.

(b) Trade-off between vehicles and bicycles.

Fig. 8. Sensitivity of controller performance against changes in the demand value – MPC Case 1.
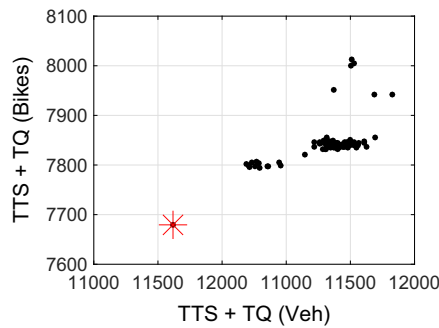

Fig. 9. MPC Case 1: for different values of α, TTS + TQ for vehicles versus bicycles.

the average. From the figure, in the "MPC Case 1" there is a single point in the Pareto front, at $\alpha = 0.11$. This is not usually the case in multiobjective analysis, as it will be shown for MPC Case 2 and MPC Case 3, where Pareto sets with multiple values of α are obtained. In those cases, the α value can be selected taking into account different criteria, finding a reasonable trade-off between the two objectives proposed in (25).

Fig. 10 shows the evolution of the number of vehicles (Fig. 10(a)) and bicycles (Fig. 10(b)) throughout the simulation (in both figures the label "MPC Case 1" stands for the MPC controller). In this figure, it can be seen that all controllers performs similarly. Indeed, only the so called open loop exhibited a significant loss of performance in comparison with the other three. This is more evident in the case of vehicles than in the case of bicycles, where all controllers performed almost the same (differences just appear after $k_d = 10$ h). It is important to notice that as the number of vehicles in the network grows, the congestion increases, and therefore the traffic system is closer to its collapse. The same claim is also valid for bicycles.

Associated with the number of vehicles and bicycles in the network, and thus with the congestion, is the formation of queues. Fig. 10 presents the evolution of the number of vehicles (Fig. 10(c)) and bicycles (Fig. 10(d)) waiting in a queue of the traffic network. The number of vehicles waiting in a queue was computed as the sum of all queues of vehicles/bicycles in the network. In accordance with the result shown in Fig. 10, there are only significant differences with respect to the open loop controller. The remaining three strategies, namely, fixed time, state-feedback, and MPC performed almost the same, the greatest difference with respect to the open loop controller being in the number of vehicles waiting in a queue. In the case of the bicycles, the differences among the controllers just appeared after $k_d = 10$ h.

4.2. MPC Case 2: Measured demand

In this section, the demand shown in Fig. 4 is assumed to be measured. At each time step k_d the inflow demands of vehicles and bicycles are known but not its evolution, i.e., the demand is not predictable. Hence, in order to carry out the prediction of the behavior of the network, MPC Case 1 will assume the demand equal to its measured value and constant during the prediction horizon. In order to find the appropriate values for α, several simulations were made to evaluate the performance of vehicles and bicycles. The results are shown in Fig. 11 and $\alpha = 0.11$ is marked in the figure. The selected α gives full priority to the vehicles. However, the methodology is generic and a different α belonging to the Pareto front could be used in benefit of the cyclists.

In Fig. 12 the evolution of the number of vehicles (Fig. 12(a)) and bicycles (Fig. 12(b)) in the traffic network is presented (here, the label "MPC Case 2" stands for the MPC controller). As it can be noticed in Fig. 12(a), the knowledge of the value of
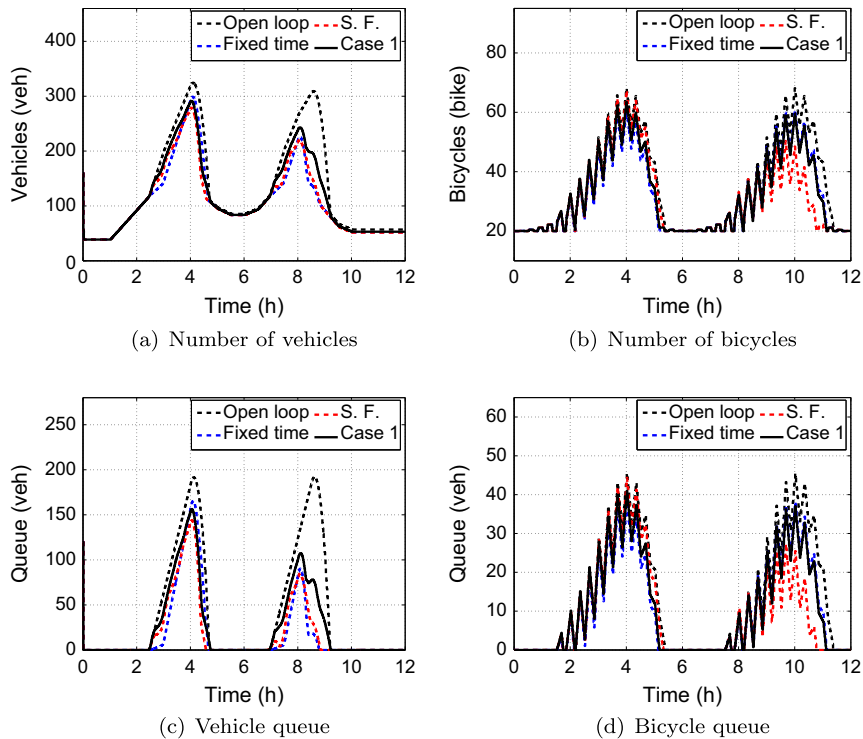
Fig. 10. Number of bicycles and vehicles for open loop, fixed time, state feedback (S.F.) and MPC Case 1 controllers. (a) Number of vehicles, (b) number of bicycles, (c) queue of vehicles, and (d) queue of bicycles.
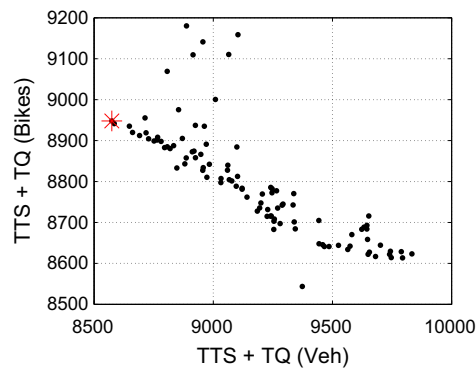

Fig. 11. MPC Case 2: Trade-off between vehicles and bicycles for different values of α.

the demand significantly improved the performance of the MPC controller. Indeed, with respect to the other three controllers, the MPC reduced the number of cars almost with a 50% during the first peak of demand. In the second peak of demand, fixed time, state-feedback, and MPC controllers performed almost the same. Also, with respect with the result shown in Fig. 10(a), the improvement of MPC was considerable. Almost a reduction of 50% was achieved by including the measured value of the demand. However, despite the improvement for the vehicles, the behavior for the bicycles remained the same. In fact, the number of bicycles with MPC tended towards the number of bicycles with the open loop strategy. This is due to the way the demand of bicycles behaves. As shown in Fig. 4(b), the demand of bicycles is less smooth and less predictable than the demand of vehicles. Thus, the currently measured value provides little information about how the demand of bicycles is expected to be.

A similar behavior can be noticed in the number of vehicles/bicycles waiting in a queue. As for the number of vehicles in the network, including the measured value of the demand allowed a reduction of 50% in the number of vehicles in the first peak of demand, whereas the behavior during the second peak was almost the same for the fixed time, state-feedback, and MPC controllers. Furthermore, in comparison with the results shown in Fig. 10(c) a reduction of 50% was also accomplished
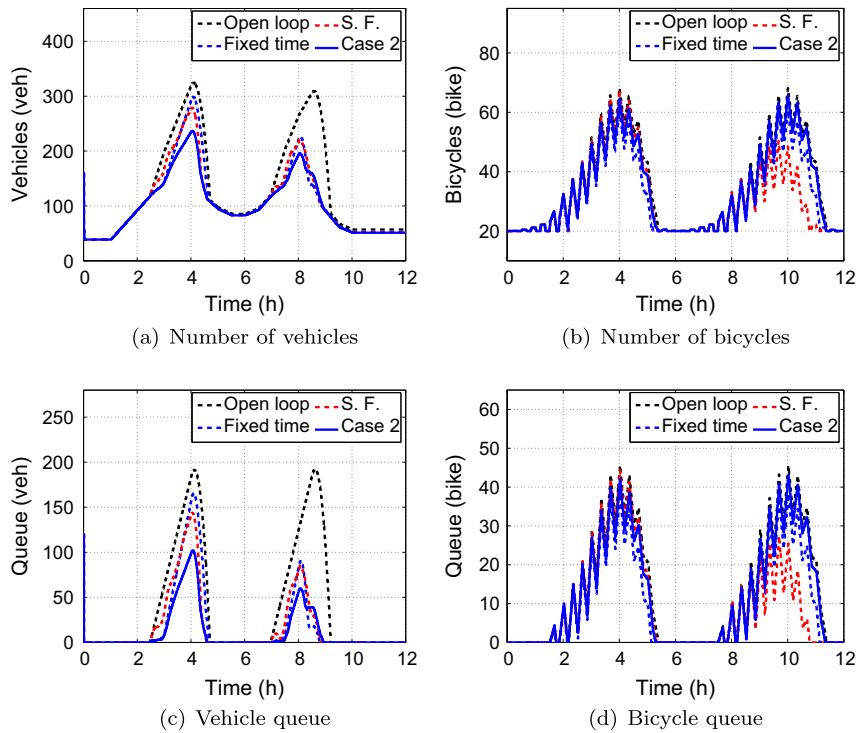
Fig. 12. Number of bicycles and vehicles for open loop, fixed time, state feedback (S.F.) and MPC Case 2 controllers. (a) Number of vehicles, (b) number of bicycles, (c) queue of vehicles, and (d) queue of bicycles.

in the number of vehicles during both peaks of demand, namely, at 4 and 8 h. Nevertheless, as expected from the results in Fig. 12, in comparison with the previous case, a slight improvement is observed in the behavior of the vehicles (Fig. 12(c)) and bicycles (Fig. 12(d)) waiting in a queue when the demand is assumed measured in the MPC controller.

4.3. MPC Case 3: Predictable demand

In this section, in addition to the possibility of measuring the demand it is assumed that the function describing the demand profiles shown in Fig. 4 is known. That is, given the measured demand it is possible to perfectly estimate its behavior several time steps ahead. In order to select the parameter α for this case, several simulations were made to evaluate the performance of vehicles and bicycles. The results are shown in Fig. 13 where an $\alpha = 0.1$ that benefit the most to the vehicles is marked.

Fig. 14 shows the results obtained in the simulations (here the label "MPC Case 3" stands for the MPC controller). In comparison with the case shown in Fig. 10, the performance definitely is improved. But, notwithstanding the additional information provided by the demand estimation, the results obtained are only slightly different from the results presented in
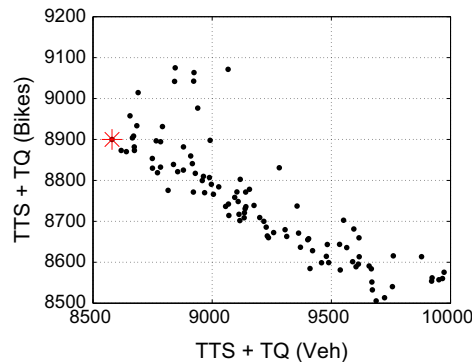

Fig. 13. MPC Case 3: Trade-off between vehicles and bicycles for different values of α.
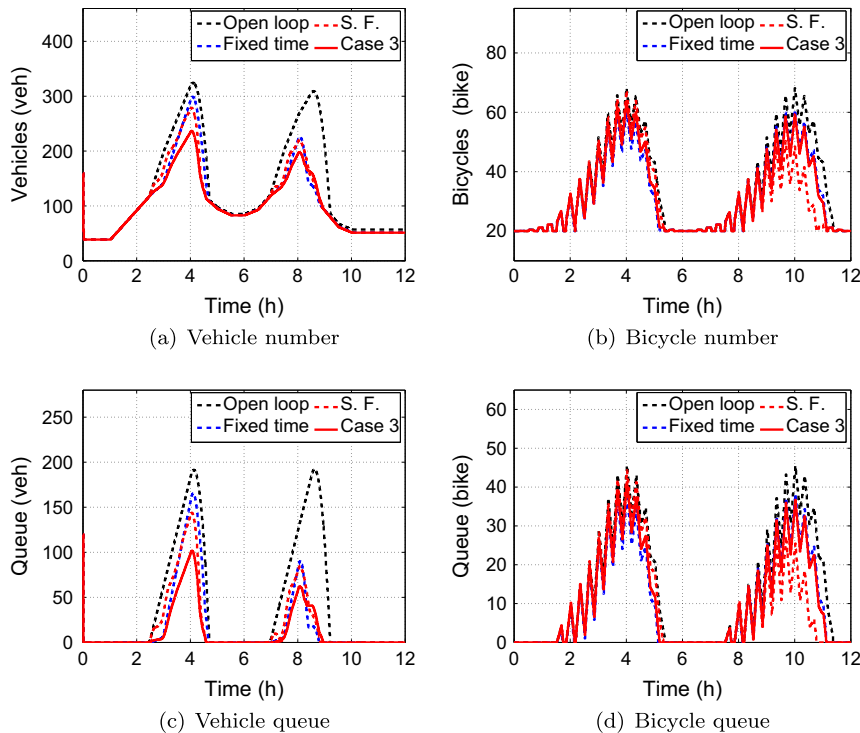
Fig. 14. Number of bicycles and vehicles for open loop, fixed time, state feedback (S.F.) and MPC Case 3 controllers. (a) Number of vehicles, (b) number of bicycles, (c) queue of vehicles, (d) queue of bicycles.

Fig. 12. In fact, the difference between those two results is in the number of bicycles during the second peak of demand. In this case, perfectly estimating the demand allowed reducing the number of bicycles to the same level shown in Fig. 10.

Fig. 14 presents the behavior of the vehicles (Fig. 14(c)) and bicycles (Fig. 14(d)) waiting in a queue, when the demand shown in Fig. 4 is perfectly estimated. Similar as in the case of the number of vehicles/bicycles in the network, in this figure the main differences are in the number of bicycles in the queues. In this case the number of bicycles was reduced in comparison with the results presented in Fig. 12(d). As for the number of bicycles in the network, the estimation allowed to achieve a similar number of bicycles as in Fig. 10(d).

Table 1 summarizes the results presented in Sections 4.1,4.2,4.3. Here, the improvement was computed in two steps: first the TTS for bicycles and vehicles of each controller was added up; then, the relative deviation with respect to the result for the open loop controller was calculated for each of the remaining controllers. In this table the improvement and deterioration of the MPC are evident additional information is added. For instance, as it can be seen the TTS of vehicles decreases from MPC Case 1 to MPC Case 2, and remains constant from MPC Case 2 to MPC Case 3. This implies that adding information enhances the performance of the controller.

However, analyzing the TTS for the bicycles it can be noticed that, as mentioned in Section 4.2, the addition of the measurement of the demand increases the TTS, but with the perfect estimation of the demand the TTS decreases nonetheless. The use of the perfect estimation of demand just produced the same result as if the bicycles demand were considered fixed, with a value over its expected average (similar statements apply for the TQ index). This situation has to do with the selection of the parameter α, which was chosen in benefit of the vehicles. Besides, analyzing the percentage of improvement with respect to the open loop controller, MPC Case 2 and MPC Case 3 MPC controllers yield the highest improvements. Fig. 15 also support

Table 1
Performance comparison of TTS and TQ for each scenario in the MPC cases. Improvement is presented with respect to open loop case.

Scheme	TTS (veh h)	TTS (bike h)	TQ (veh)	TQ (bike)	Improvement %	
					TTS	TQ
Open loop	792.21	209.90	28.682	9.568	–	–
Fixed time	646.94	190.90	12.781	7.289	16.39	47.53
State Feedback	647.71	186.15	13.085	6.718	16.79	48.23
MPC Case 1	693.04	192.99	18.041	7.538	11.58	33.12
MPC Case 2	608.91	201.68	8.512	8.582	19.11	55.31
MPC Case 3	609.37	192.13	8.579	7.436	20.02	58.13

(a) Number of vehicles

(b) Number of Bicycles

(c) Vehicle queue

(d) Bicycle queue

Fig. 15. Number of bicycles and vehicles.

(a) Stage 1 of intersection u

(b) Stage 2 of intersection u
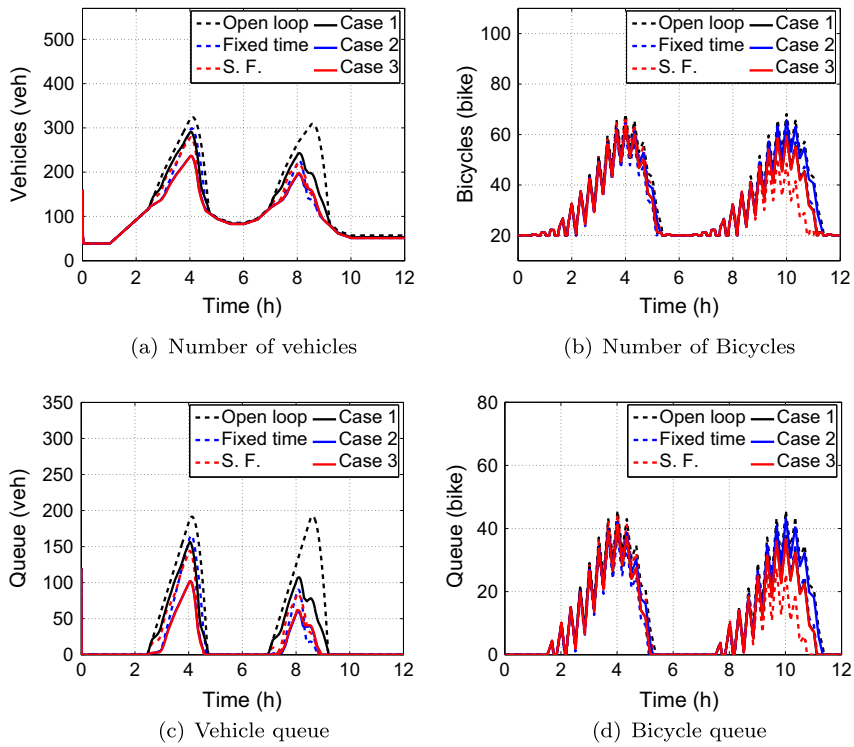
(c) Stage 1 of intersection d
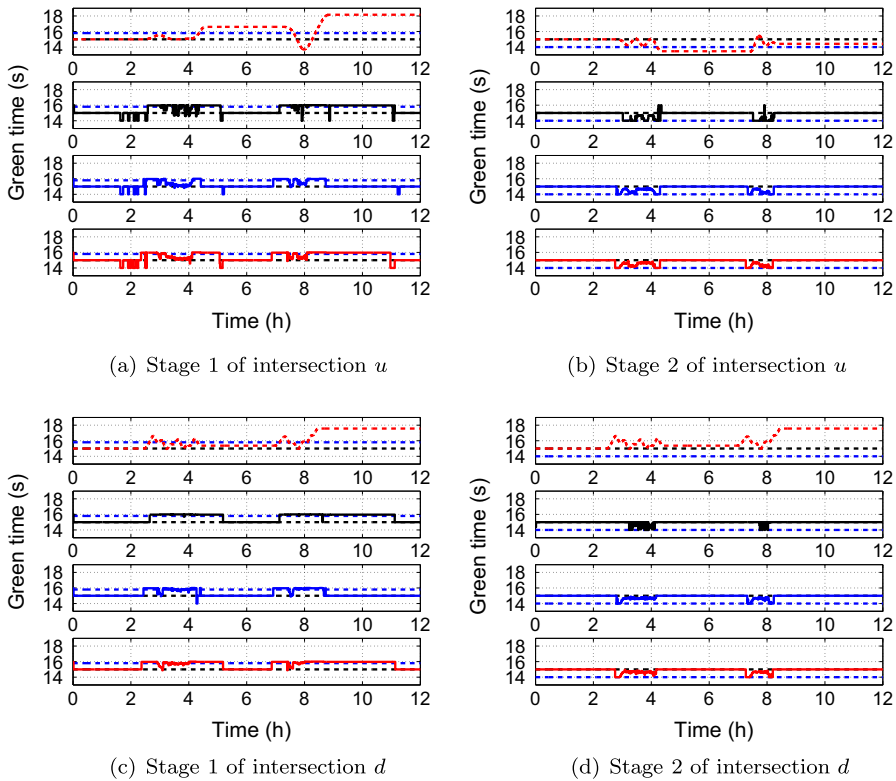
(d) Stage 2 of intersection d

Fig. 16. Control actions stage 1 and stage 2, for the intersections u and d.

these statements. A real-life implementation of MPC Case 3 would require a very sophisticated model that exactly predicts the future demands, probably combining off-line historical information with on-line measurements of the inflow demands. MPC Case 2 would only require the installation of inflow demand sensors.

Despite the similarities among the responses of the controllers, there still are some differences among them. For instance, the control actions applied to the system. Fig. 16 presents the control actions applied by each of the controllers previously analyzed (this figure has the same legends as Fig. 15). Specifically, stages 1 and 2 of intersections *u* (Fig. 16(a) and (b) respectively) and *d* (Fig. 16(c) and (d) respectively) are shown. As it can be noticed in this figure, controllers with similar performance in terms of TTS and/or TQ applied different control actions. In particular, the perfect estimate of the demand reduced the high variations of the control actions by MPC. The use of the measured demand in the predictions produced a similar effect on MPC labeled "MPC Case 2", but the changes in the control actions are more evident. From these statements it can be concluded that using the wrong demand causes more variations in the control signals. Further concluding remarks and discussion of the results are given in the next section.

5. Conclusions

In this paper, we have incorporated explicitly the dynamic effect of bicycling in a systematic methodology to control multi-modal traffic lights based on a model predictive control approach. The case studies presented show the importance for MPC of measuring or estimating both, the vehicle demand and bicycle demand. In "MPC Case 1" traffic demand is not measured, producing a low controller performance. When the demand is measured ("MPC Case 2"), the controller improves performance considerably. Finally, in "MPC Case 3" the demand is known and it has the best performance. However, real-life implementation of "MPC Case 3" would require a sophisticated model to accurately predict the demand value.

The inclusion of bicycling in the urban traffic faces various challenges. Limited knowledge is available about cycling flows and models at all the levels of bicycling, from cyclist behavior, activity scheduling, route choices, learning mechanisms of optimal routes, interaction with automobiles when separate cycle paths are not available. Interaction with the infrastructure, not just at the level of traffic lights, but also with parking facilities, combination of private and shared-bikes platforms, electric bikes for difficult high slopes and the use of crowdsourcing data of cyclists are some of the topics of further research.

Although bicycle flow theory is in its early stage of development, we believe that the integration of new bicycle models, including social, temporal, and spatial characteristics is very important to facilitate the integration of cyclists in the multi-modal network. Models such as continuum models, discrete models, and game theory models can enhance the decision making of the MPC and increase the level of service from the cyclists' point of view.

Acknowledgements

References

Budnitzki, A., 2014. Computation of the optimal tolls on the traffic network. Eur. J. Oper. Res. 235 (1), 247–251.

Burger, M., van den Berg, M., Hegyi, A., De Schutter, B., Hellendoorn, J., 2013. Considerations for model-based traffic control. Transp. Res. Part C 35, 1–19.

Camacho, E., Bordons, C., 1999. Model Predictive Control. Springer-Verlag, London.

Cesme, B., Furth, P.G., 2014. Self-organizing traffic signals using secondary extension and dynamic coordination. Transp. Res. Part C: Emerging Technol. 48, 1–15.

Cheng, S., Su, Y., Yao, D., Zhang, Y., Li, L., Teng, R., 2008. A CA model for intrusion conflicts simulation in vehicles-bicycles laminar traffic flow. In: Proceedings of the 11th International IEEE Conference on Intelligent Transport Systems. Eindhoven, Netherlands, pp. 727–732.

Daganzo, C.F., 1995. The cell transmission model, part ii: network traffic. Transp. Res. Part B: Methodol. 29 (2), 79–93.

Darby, M.L., Nikolaou, M., 2012. MPC: current practice and challenges. Control Engineering Practice 20(4), 328–342, Special Section: IFAC Symposium on Advanced Control of Chemical Processes – ADCHEM 2009.

Dijkstra, A., 2012. Effecten van een robuust wegennet op het fietsverkeer. Tech. Rep., Stichting Wetenschappelijk Onderzoek Verkeersveiligheid SWOV, Leidschendam (in Dutch).

Fahad, A., Tari, Z., Khalil, I., Almalawi, A., Zomaya, A.Y., 2014. An optimal and stable feature selection approach for traffic classification based on multi-criterion fusion. Future Gener. Comput. Syst. 36, 156–169.

Gatersleben, B., Haddad, H., 2010. Who is the typical bicyclist? Transp. Res. Part F: Traffic Psychol. Behav. 13 (1), 41–48.

Guizhu, W., Bing, L., 1997. Automatic detecting system for traffic flow of bicycles based on pattern recognition and classification. In: Proceedings of the 1997 IEEE International Conference on Systems, Man, and Cybernetics. Computational Cybernetics and Simulation, vol. 5. Orlando, USA, pp. 4360–4363 (12–15 October).

Guler, S.I., Menendez, M., Meier, L., 2014. Using connected vehicle technology to improve the efficiency of intersections. Transp. Res. Part C: Emerging Technol. 46, 121–131.

He, Q., Head, K.L., Ding, J., 2012. PAMSCOD: platoon-based arterial multi-modal signal control with online data. Transp. Res. Part C: Emerging Technol. 20 (1), 164–184.

He, Q., Head, K.L., Ding, J., 2014. Multi-modal traffic signal control with priority, signal actuation and coordination. Transp. Res. Part C: Emerging Technol. 46, 65–82.

Hegyi, A., De Schutter, B., Hellendoorn, H., 2005. Model predictive control for optimal coordination of ramp metering and variable speed limits. Transp. Res. Part C 13 (3), 185–209.

Jamshidnejad, A., Papamichail, I., Papageorgiou, M., De Schutter, B., 2015. Model-Predictive Control for Green Mobility in Urban Traffic Networks: Efficient Solution Based on General Smoothening Methods. Tech. Rep. 15-033, Delft Center for Systems and Control, Delft University of Technology, Delft, The Netherlands (submitted for publication).

Le, T., Vu, H., Nazarathy, Y., Vo, B., Hoogendoorn, S., 2013. Linear-quadratic model predictive control for urban traffic networks. Procedia – Soc. Behav. Sci. 80, 512–530.

Lee, J.H., 2011. Model predictive control: review of the three decades of development. Int. J. Control Autom. Syst. 9 (3), 415–424.

Li, Z., Elefteriadou, L., Ranka, S., 2014. Signal control optimization for automated vehicles at isolated signalized intersections. Transp. Res. Part C: Emerging Technol. 49, 1–18.

Lin, S., De Schutter, B., Xi, Y., Hellendoorn, H., 2011. Fast model predictive control for urban road networks via MILP. IEEE Trans. Intell. Transp. Syst. 12 (3), 846–856.

Lin, S., De Schutter, B., Xi, Y., Hellendoorn, H., 2012. Efficient network-wide model-based predictive control for urban traffic networks. Transp. Res. Part C 24, 122–140.

Parkin, J., Meyers, C., 2010. The effect of cycle lanes on the proximity between motor traffic and cycle traffic. Accid. Anal. Prevent. 42 (1), 159–165.

Schmöcker, J.-D., Ahuja, S., Bell, M.G., 2008. Multi-objective signal control of urban junctions – Framework and a London case study. Transp. Res. Part C: Emerging Technol. 16 (4), 454–470.

Shen, W., Zhang, H., 2014. System optimal dynamic traffic assignment: properties and solution procedures in the case of a many-to-one network. Transp. Res. Part B: Methodol. 65, 1–17.

U.S. Department of Transportation, 2010. The National Bicycling and Walking Study: 15-Year Status Report.

van den Berg, M., De Schutter, B., Hegyi, A., Hellendoorn, J., 2004. Model predictive control for mixed urban and freeway networks. In: Proceedings of the 83rd Annual Meeting of the Transportation Research Board. Washington, DC, paper 04-3327.

van den Berg, M., Hegyi, A., De Schutter, B., Hellendoorn, J., 2003. A macroscopic traffic flow model for integrated control of freeway and urban traffic networks. In: Proceedings of the 42nd IEEE Conference on Decision and Control. Maui, Hawaii, pp. 2774–2779.

Wu, X., Liu, H.X., 2014. Using high-resolution event-based data for traffic modeling and control: an overview. Transp. Res. Part C: Emerging Technol. 42, 28–43.

Zhang, L., Yin, Y., Chen, S., 2013. Robust signal timing optimization with environmental concerns. Transp. Res. Part C: Emerging Technol. 29, 55–71.